ARTICLES

Molecular Dynamics of Hydrogen Bonds in Protein−D_2O: The Solvent Isotope Effect

Sheh-Yi Sheu,*,†,‡ E. W. Schlag,*,†,§ H. L. Selzle,§ and Dah-Yen Yang*,†,#

Department of Life Sciences, National Yang-Ming University, Taipei 112, Taiwan, Institute für Physikalische und Theoretische Chemie, TU-München, Lichtenbergstrasse 4, 85748 Garching, Germany, and Institute of Atomic and Molecular Science, Academia Sinica, Taipei 106, Taiwan

Received: September 6, 2007

We suggest that the H-bond in proteins not only mirrors the motion of hydrogen in its own atomistic setting but also finds its origin in the collective environment of the hydrogen bond in a global lattice of surrounding H_2O molecules. This water lattice is being perturbed in its optimal entropic configuration by the motion of the H-bond. Furthermore, bonding interaction with the lattice drop the H-bond energy from some 5 kcal/mol for the pure protein in the absence of H_2O, to some 1.6 kcal/mol in the presence of the H_2O medium. This low value here is determined in a computer experiment involving MD calculations and is a value close to the generally accepted value for biological systems. In accordance with these computer experiments under ambient conditions, the H-bond energy is seriously depressed, hence confirming the subtle effect of the H_2O medium directly interacting with the H-bond and permitting a strong fluxional behavior. Furthermore, water produces a very large change in the entropy of activation due to the hydrogen bond breakage, which affects the rate by as much as 2 orders of magnitude. We also observe that there is an entire ensemble of H-bond structures, rather than a single transition state, all of which contribute to this H-bond. Here the model is tested by changing to D_2O as the surrounding medium resulting in a substantial solvent isotope effect. This demonstrates the important influence of the environment on the individual hydrogen bond.

I. Introduction

The dynamics of protein folding and enzymatic reaction is intrinsically related to the strength of the hydrogen bond. The breaking and making of the hydrogen bond is one of the key steps in all protein motion. The dynamics of this motion is one of the most decisive factors determining protein structure in solution, lipid membranes, and other environments.

Structural properties of proteins are known to display solvent isotope effects though the details of the mechanisms are in general not known.[1−5] This effect has been observed for many slower processes in proteins, such as folding studies from NMR, H/D exchange or fluorescence studies processes. Many microscopic contributions are here displayed in the overall process.

The primary and immediate origin of these structural factors in proteins that are contributing to the making and breaking hydrogen bonds are not known. It is of interest to look for a possible direct connection between the solvent and the primary hydrogen bond by directly observing the process on a picosecond time scale using molecular dynamics.

It is now well-established that under typical conditions these H-bonds are not rigid but rather fluxional on a time scale of some 50 ps. Such fluxional bonding processes are important for many biological processes involving protein motions, in folding, or in the chemistry of enzymes. This fluxional behavior is due to the very low activation energy of such H-bond ruptures of some 1−1.5 kcal/mol, as has been known for some time. Any higher energy would not lead to fluxional motions due to the low value of *RT* (thermal energy term) in biological systems, and hence the absence of such motions would not support many life processes. Previous molecular dynamics calculations also confirm such low activation energies, particularly in H_2O.

In the absence of water we note considerably higher activation energies (Table 1) that are of less biological interest because physiological temperatures here do not lead to ruptures and realignments as seen in protein dynamics. We directly observe the presence of such higher energy intra H-bonds in our system (Figure 3), which, however, give way to the normal H-bonds at a much lower energy in the water environment. The solvent environment is seen to dominate the hydrogen bond rupture process, orientation and energetics. In the solvated system, the protein is wrapped by a fluctuating water cavity (or clathrate hydrates).[6−12] It is the intraprotein H-bond rupture dynamics that is suppressed by the entropy changes of this cavity. In vacuum, the protein side chain prefers to form intramolecular H-bonds.[13] However, in the water system, the side chain extrudes into water and interacts with the solvation environment reducing the energy needed to rupture. At the same time water reduces the rate by some 2 orders of magnitude, due to the very large changes in entropy produced by the rupture process. The inner hydrogen bond pair is protected by the protein from activation. These two factors actually compete with each other.

* To whom correspondence may be addressed. E-mail: S.-Y.S., sysheu@ym.edu.tw; E.W.S., schlag@ch.tum.de; D.-Y.Y., dyyang@po.iams.sinica.edu.tw.

† S.-Y.S., E.W.S., and D.-Y.Y. contributed equally to this work.

‡ National Yang-Ming University.

§ TU-München.

Academia Sinica.

10.1021/jp0771668 CCC: $40.75
Published on Web 01/15/2008

TABLE 1: Prefactor (s^{-1}) and Activation Energy (kcal/mol) of the Hydrogen Bond Rupture Processes in Various Phases

	in vacuum		in D_2O		in H_2O	
	H^+_{BA}	A	H^+_{BA}	A	H^+_{BA}	A
α-helix	5.55	5.02×10^{13}	3.61	5.01×10^{12}	1.93	5.49×10^{11}
β-hairpin	4.79	9.37×10^{12}	3.07	1.73×10^{12}	1.58	3.53×10^{11}

Some intrinsic properties of the differences of H_2O and D_2O have been known for quite a long time.[14] Though the normal water and heavy water taste the same, there are still several physical properties that are different between these two molecules such as viscosity, melting point, the temperature of maximum density and the heat capacity.[15] For example, the D_2O melting point is 3.82 °C and its boiling point is 101.4 °C. So the heavy water ice may sink in regular water and the D_2O ice will not melt in ice-cold normal water. Furthermore, the pH-value of regular water is 7.0 and the pD-value of D_2O is 7.41 at room temperature. More interesting is the molecular dimensionality and dipole interaction of D_2O, which are almost identical to that of H_2O. But D_2O has a stronger O−D···O bond energy (here termed a D-bond) than that of H-bond in H_2O. These make liquid D_2O more structurally ordered than H_2O at a given temperature. D_2O is also considered a better solvent for NMR studies of biological molecule than H_2O due to their nuclear spin difference. Protein unfolding entropy and enthalpy are hence significantly reduced in D_2O.[16−18]

Living cell division is usually disrupted by D_2O. The well-known eukaryotic cell division is stopped in D_2O and plants also cease to grow in D_2O. A small animal such as the tadpole can be killed by high concentration heavy water. It is obvious that heavy water dramatically influences the biological system. A microscopic understanding of the protein hydrogen bond may be due to the D_2O solvation processes.[19−26]

The making and breaking of H-bonds in proteins is fluxional on a 50 ps time scale and as such, this behavior is essential for many dynamic biological processes. Here we suggest that these fluxional motions do not reflect the atomic motion of a single bond but rather reflect a collective motion that can only be operative in conjunction with the large surrounding network of water molecules as a whole. The breaking of an H-bond is a collective network property, and not the property of any individual bond. The energetics observed here is in very close analogy to recent thinking on the dynamics and energetics of water networks.[27] In fact, such global water processes may be rate determining for our hydrogen bond kinetics as well.

The rupture of an H-bond is often described in terms of a transition state. In terms of classical transition state theory (TST)[28] it is not certain if such a concept can easily be applied to the H-bond because it is not clear if there is an equilibrium of transition states formed as required by TST. Detailed examinations of the various starting configurations in an MD calculation leading to H-bond rupture showed very different angles and structures in the orthogonal degrees of freedom for these various starting states. The critical state can be better described as an ensemble of configurations in which a particular distension ruptures, but these configurations do not appear to be in equilibrium. Such ensemble views without definite structures have been postulated before for water where enthalpies were determined for the ensemble without identifying specific structures.[29,30] A similar view appears to be correct here for the H-bond imbedded in water. Hence in a similar way it will be difficult to obtain energies from structural arguments or from statistical thermodynamics because again these depend on unique structures that do not appear to exist in the MD samples investigated. Furthermore, the inclusion of the observed very large entropy terms in such calculations may be difficult. Rather, a distribution of structures undergoing H-bond breaking in a computer experiment may be the most appropriate and realistic viewpoint.

In previous work we showed, by observing the mean first passage time for the H-bond rupture in an ensemble of structures, that we define a rate constant from a computer experiment. By repeating this computer experiment at a different temperature, we obtain the activation energy for the entire ensemble. Such energy does not invoke any one structure; just the critical rupture must be defined for the mean first passage time. The observed activation energy for the rupture of such an H-bonded ensemble in water was thus determined to be 1.6 kcal/mol. Such a value is generally the accepted value for biological systems.[31−33] This is very close to the value for the ensemble of structural rearrangements in pure water of 1.6 kcal/mol. Again, this similarity of values would be expected because in both cases a very similar ensemble is involved. In the case of the H-bond, the rupture disturbs the maximum entropy configuration of the water shell aggregated around the H-bond in an ensemble of different configurations. Note that in the absence of water the same system has H-bond strength of some 6 kcal/mol. It is the ensemble of water structures interacting with the H-bond that facilitates the H-bond rupture to produce and energy palatable to biological processes at typical biologically relevant temperatures. Water is required to bring the molecular value of the H-bond strength into the biologically interesting region, useful in such processes. In this work we report values for the computer experiment in D_2O, where we observe the most interesting result that little rupture is observed in the MD computer experiment. This again demonstrates that we are dealing rather with a global water interaction than with a pure atomistic model. This would be expected for such a subtle entropic effect. It is indeed well-known that many biological processes are suppressed in D_2O. The overall conclusion is that we are suggesting a different way of thinking about H-bond in proteins in the presence of a water environment. This is due to a synergetic effect between the H-bond rupture and the rearrangement of very large complex water structures around it—a rearrangement of the hydrophobic bond.

That molecules dissolved in water form clathrate hydrates structure has been known for some time and been reviewed in ref 34. These clathrate hydrates around small molecules are considered to have quite an ordered structure thus wrapping around the solute molecule and moderating the collective motion. This causes an entropic penalty to the solvation process. For a weak clathrate hydrates structure such as water, due to weaker H-bond compared to the stronger D-bond the more dynamic H_2O fluctuation can shake the intraprotein hydrogen bond rupture more severely. D_2O exhibits a stronger solvent−solvent D-bond[35,36] than H_2O has; hence D_2O may have more rigid clathrate hydrates structure.

In our previous work,[35] we studied the hydrogen bond rupture processes via a kinetic method involving a MD experiment. A time series has been used to extract out the hydrogen bond energy and the prefactor. Our MD simulation is kept under a constant pressure situation and hence the activation energy is the enthalpy. Its prefactor accounts for the entropy of the rupture process. Moreover, this prefactor agrees with the clathrate hydrates assertion. In other words, when a protein is solvated in water solution, the water molecules are repelled to form a clathrate hydrates surrounding the protein.[35] As we mentioned above, the inner hydrogen bond rupture process breaks the well-

organized water structure that exists in an entropically optimized state. The breaking process forces a total rearrangement in this organized structure and thus severely reduces the entropy. In TST formulation this would lead to a severely reduced pre-exponential factor in the Arrhenius expression.

After we introduce our kinetic method to resolve the H-bond rupture processes, we present a short connection between the Arrhenius law, transition state theory and Kramers theory. Because the exponential part of the Arrhenius equation is internal energy, the transition state theory has activation enthalpy in its activation term. The solvent dynamics effect is stored in the transmission factor, and its product with the transition state rate gives the Kramers equation. In the solution theory, the activation term contains the Gibbs free energy and the entropy effect is shown in the prefactor. These help us to study the entropy effect through the rupture processes.

II. Molecular Dynamics Simulation

To investigate the hydrogen bond rupture process, we use the CHARMM program[37] and the CHARMM22 force field[38] is employed, but here to determine rates, and not structures. Our test polypeptide α-helix with 13-mer, i.e., Ace-SDELAK-LLRLHAG-NH_2, where Ace = $-COCH_3$, is first minimized in vacuum and then is used as a starting configuration for subsequent molecular dynamics simulation. We also quote a β-hairpin 12-mer, i.e., Ace-V5PGV5-NH_2, to repeat the same simulation.

We constructed a solvated system by wrapping the polypeptide chain with 905 D_2O molecules for the α helix and 914 D_2O molecules for the beta-sheet. Because the force constant for D_2O is the same as H_2O, the difference between D_2O and H_2O is the mass term. Therefore, the TIP3P water model[33] is used and we modify the mass of H by D, as a result some of the corresponding harmonic force constant are also changed. The entire molecular dynamics simulation is performed up to 0.5 ns. To illustrate the rupture processes, the time series of the N−O distance of each hydrogen bond pair is counted.

The traditional method used to compute the free energy is to sum over all energy fluctuations. During the summation, all of the bond-breaking processes are averaged out, i.e., ensemble average. This is the so-called thermodynamics method. For the protein solvation processes there are many bond rupture and formation processes. To compare the detailed microscopic processes, we have to count individual processes, which gives us specific bond rupture information and warrants our counting of the correct events. The other way of estimating the transition rate is through a kinetic method we introduced in our previous work.[31−33] A classical transition state theory estimates the transition rate by counting a successful trajectory as climbing from a minimum in the well and proceeding to the barrier top. In our method, the activation energy is extracted via a computer experiment finding the mean first passage of the bond distension. We observe the microscopic hydrogen bond dissociation and formation processes in a computer experiment. From this we obtain a mean first passage time and hence the activation energy as well as the rarely determined entropy contribution to the rate.

Activation Thermodynamics. Here we evaluate the mean first passage time of the hydrogen bond rupture using molecular dynamics directly from a computer experiment. Because our H-bond energy is extracted from a time series of such H-bond rupture processes, we can fit the rupture rate with the Arrhenius equation directly yielding several important thermodynamic quantities. We want to briefly review the entropy effect and Gibbs free energy of the activation processes in a solvation system.

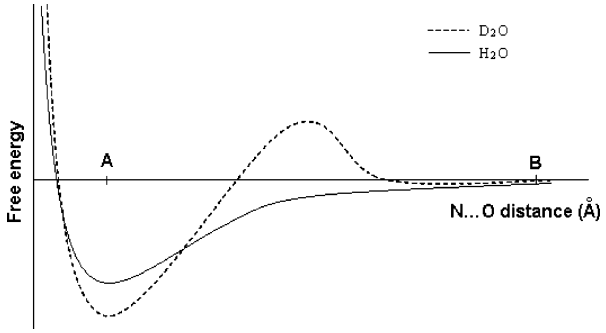

Figure 1. Hydrogen bond rupture process. Here we show the rupture time of hydrogen bond break in water system (solid line). Comparing the same hydrogen bond pair in D_2O (dash line). Presumably, the free energy surface of protein in D_2O is compressed to have a higher curvature in well A and a higher barrier B.

Experimentally measured rate constants can be used to extract the thermodynamic information, but basically we fit the data with the Arrhenius equation first instead of using transition state theory or Kramers theory. We therefore review and distinguish the basic thermodynamic energies in the activation process. These fundamental thermodynamic quantities are connected to the experimental results indirectly.

A. Arrhenius Equation. Typically, a reaction rate, no matter whether in the gas phase or in the solvated system, depends on many parameters such as temperature, friction and pressure etc. Experimentally, we can extract the thermodynamic energy from the Arrhenius equation $k = Ae^{-E_a^+/k_BT}$. Here the prefactor A is essentially temperature independent. But the activation energy E_a^+, an internal energy of the reaction, dominates the temperature-dependent effect; k_B is the Boltzmann constant. According to the measured reaction rates, prefactor A-value and E_a^+ are obtained by plotting log k versus $1/T$ (Arrhenius plot). Other related activation thermodynamic quantities can then be obtained.

B. Transition State Theory. Now we first consider a gas-phase rate theory in Figure 1 as an example where E_a^+ indicates the barrier height between the well A and the dissociation state B. We also assume the system to be in equilibrium at the temperature T. The molecules vibrate in well A (Figure 1) with a frequency given by $\nu = k_BT/h$ about 10^{13} s^{-1} at 300 K. Therefore, the transition state rate satisfies $k_{TST} = \nu Ze^{-E_a^+/k_BT}$, where Z is the ratio of (number of states or degeneracy on the dissociation state)/(the number of states in well A) and is equal to $e^{S_a^+/k_B}$ where S_a^+ is the entropy difference between the well and the transitionn state. Consequently, we obtain $k_{TST} = \nu e^{-F_a^+/k_BT}$, where $F_a^+ = E_a^+ - TS_a^+$ is the difference in Helmholtz energy between well A and dissociation states, which is the activation Helmholtz energy, assuming that the experiment is done under a pressure P and the volume of the system is V_A in state A and V_{AB} at the dissociation state. The particle moving from well A to the dissociation state requires an energy $E_{AB} + PV_{AB}^+$, with $V_{AB}^+ = V_{AB} - V_B$, to reach the dissociation state, where V_{AB}^+ is called the activation volume. We then have the activation enthalpy, $H_{AB}^+ = E_{AB}^+ + PV_{AB}^+$. The final expression of the transition state rate constant now obeys $k_{TST} = \nu e^{-G_{AB}^+/k_BT}$ with the activation Gibbs free energy $G_{AB}^+ = H_{AB}^+ - TS_{AB}^+$ and $A = \nu e^{S_{AB}^+/k_B}$. By using $\nu = k_BT/h$, we have the Eyring expression $k_{TST} = k_BT/he^{-G_{AB}^+/k_BT}$. For the gas-phase reaction, because $PV = nRT$, where n is the molar number, R is the gas constant, we obtain the PV difference between well A and dissociation state as $\Delta(PV) = \Delta nRT$. Here Δn is the molar

number difference during the reaction. For the dissociation reaction C → A + B, then Δn is equal to 1. We finally have $E_a^+ = H_{AB}^+ - RT$, and the activation entropy $S_{AB}^+ = R \ln A - R \ln T - R \ln k_B/h$ is obtained by a fitted A-value.

C. Kramers Theory. Chemical reaction in a solvent has a more complicated behavior, and the easiest way to include this solvent dynamic effect is to adopt the Kramers theory. A phenomenological friction is included in this theory. Before we introduce the Kramers theory, it is useful to introduce some terminology. Here the relationship between velocity autocorrelation time τ_v and the friction coefficient ζ is established in $\tau_v = m/\zeta$ where m is the particle mass. Based on the Stokes law, a simple relationship exists between viscosity η and friction, i.e., $\zeta = 6\pi\eta a$, where a is the particle radius. The effect of friction can be characterized by a transmission coefficient $\kappa = \kappa k_{TST}$. Here κ includes the solvent dynamic effects. Comparing the rate constant with friction to the Arrhenius equation, we obtain $\kappa = \kappa\nu e^{-G_{AB}^+/k_BT} = Ae^{-\varepsilon_{AB}^+/k_BT}$. Because E_a^+ is the internal energy, the prefactor for a chemical reaction in solution is then equal to $A = \kappa\nu e^{S_{AB}^+/k_B - \Delta(PV_{AB}^+)/k_BT}$. For unitary reaction, A ⇄ B, the activation volume is almost fixed; hence we can approximate $\Delta(PV_{AB}^+) \sim 0$. We therefore get the thermodynamic quantities as $E_a^+ = H_{AB}^+ - \Delta(PV_{AB}^+) \approx H_{AB}^+$, and $S_{AB}^+ = R \ln A - R \ln \kappa - R \ln T - R \ln k_B/h$. One then can obtain the activation energy and the prefactor through the Arrhenius fit. Hence we can obtain H_{AB}^+ and S_{AB}^+. The most interesting Gibbs free energy then satisfies the relationship $G_{AB}^+ = H_{AB}^+ - TS_{AB}^+$.

According to the Gibbs free energy, the entropy effect for the unitary reaction is included in the prefactor part. A typical prefactor value is ca. 10^{13} s^{-1}. Solvent dynamics effect can change the entropy and thus lower the A-value and the prefactor.

Kinetic Method. We here assume that the protein hydrogen bond rupture processes follows a dynamic process inside a typical dissociation curve for the unitary reaction (Figure 1). At point A the hydrogen bond stays at its equilibrium state and its typical distance is ca. 2.0 Å. Because the peptide chain fluctuates until the hydrogen bond distance increases to 3.5 Å, i.e., point B. We count this as a rupture process. This is due to its similarity to a Brownian particle climbing a high barrier. We follow Yamamoto's correlation function method, i.e., a microscopic average of the fluctuation−dissipation theorem of

$$k(t) = \frac{\langle h_A(x(0) \cdot h_B(x(t)\rangle}{\langle h_A(x(0)\rangle} \approx k_{A\to B} \exp(-t/t_{rxn}) \qquad (1)$$

Here $h_A(x(0))$ is a characteristic function that counts the number of the trajectories reaching $x(0)$ at point A; $h_B(x(t))$ in the same way counts the number of the trajectories reaching $x(t)$ at point B. Our simulation has counted the trajectory with a time scale longer than the system relaxation time t_{rxn}. We can then separate the factors of the rate constant $k_{A\to B}$ and the relaxation process from the time dependent rate constant $k(t)$. Here $x(t)$ represents a point in phase space and $\langle \ldots \rangle$ denotes the ensemble average of the phase space.

Because our molecular dynamics simulation is based on Yamamoto's picture, the measured rate constant is a microscopic ensemble average over all degrees of freedom. Our counting of the N − O distance actually averages out the bending of the NH−O angle. Also, the activation energy estimated here is different from the total energy estimated from MD simulations. Because the total energy in MD is a sum of all kinds of energies, and it does not include the dynamics. Finally, our MD simulation is performed under a constant pressure.

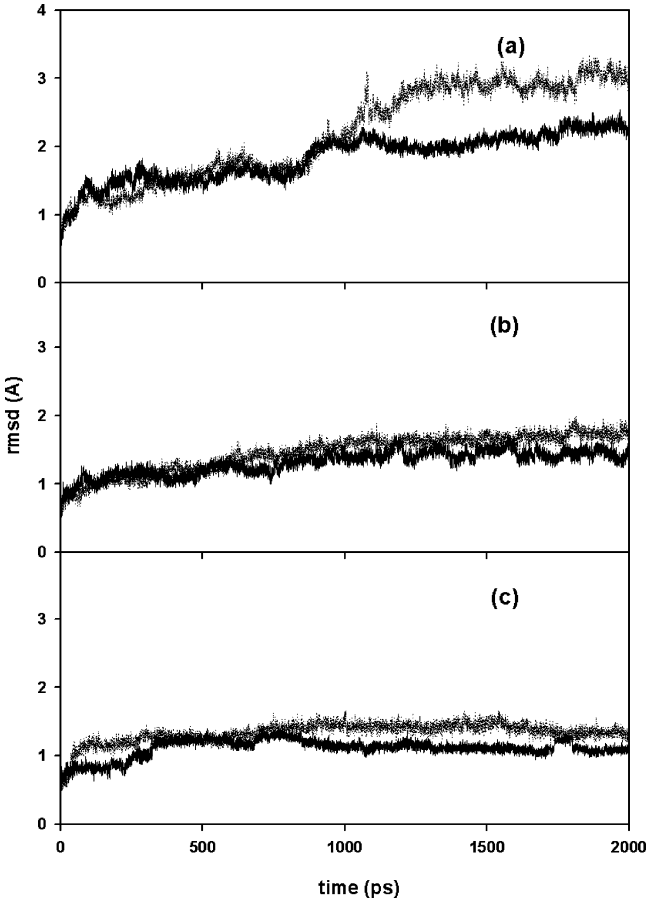

Figure 2. Comparison of the root-mean-square deviation (rmsd) in Å for α-helix configurations in D_2O (solid line) and H_2O (dot line), respectively, at (a) 330 K, (b) 300 K, and (c) 250 K. During the equilibration process, after 2 ns MD simulation, the protein rmsd in D_2O is smaller than that in H_2O. This confirms the compression of the protein in D_2O.

III. Results and Discussion

The isotope effect of water molecules shows a quite complex way for considering the hydrogen bond. Both H_2O and D_2O have the same dipole interaction. However, the frequency of exchange of the solvent molecules involved in the protein−solvent H-bond formation is strongly reduced in D_2O.[16−20] This leads to two ways of showing the suppression of the entropy effect in Kramers theory. It is clear, as we showed in the previous paragraph, the entropy effect in Kramers theory goes into the prefactor. Hence a small prefactor A-value means a large throttling effect. The second way of considering the entropy effect is through the rupture pattern, which is also changed in its amplitude.

The rupture processes of the H-bond of the protein in H_2O are depicted in Figure 1. For the dissociation process, the H-bond distance starts from point A to the barrier B point. The point B here is defined as dissociation state. Although the protein is dissolved in D_2O, due to the stronger D-bond and heavy cavity effects, the free energy surface is compressed to have a deeper well and a higher barrier as is shown in Figure 1b. These changes agree with the following arguments.

In Figure 2, the root-mean-square derivation (rmsd) of the protein in both H_2O and D_2O is depicted. At various temperatures, we show the compact structure of protein solvated in D_2O. Even though a clathrate hydrate has more difficulty to exist for a large molecule, heavy D_2O acting as hard cavity with the stronger D_2O network and D-bond compresses the protein.

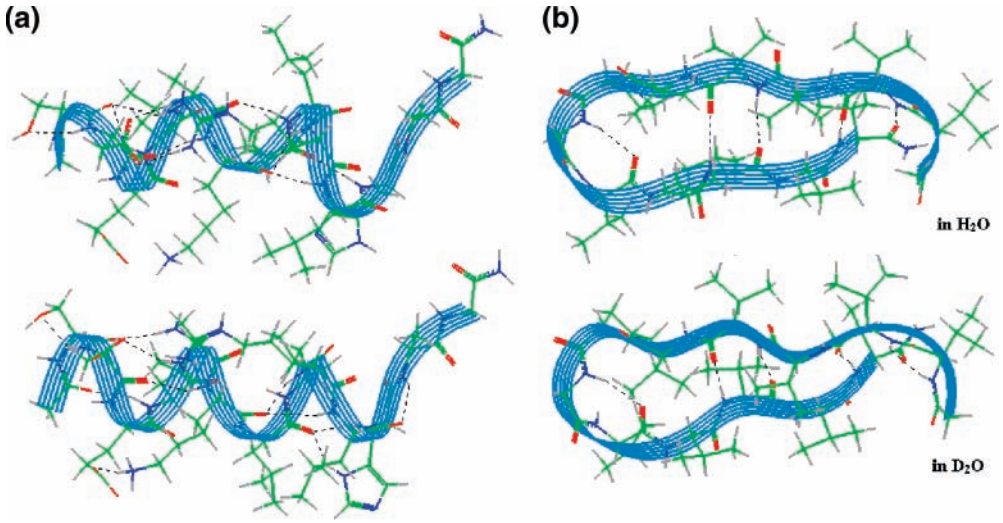

Figure 3. Snapshot of protein hydrogen bond in D_2O and H_2O for α-helix (A) and *β*-sheet (B). It is clear that for both kinds of protein, the number of intraprotein hydrogen bonds in H_2O is larger than that in D_2O. This supplements the argument in Figure 2 that the protein is more compact in D_2O than in H_2O.

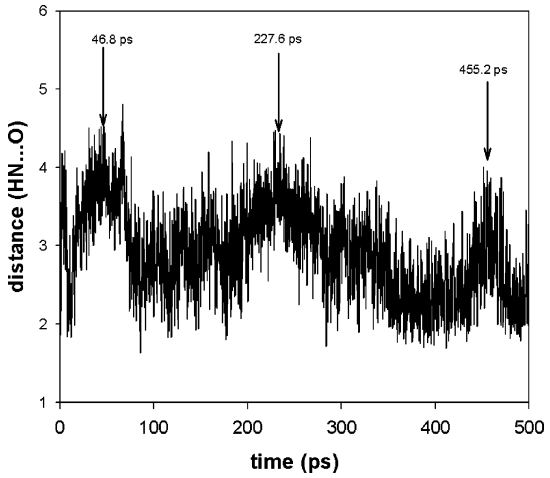

Figure 4. Time series of rupture processes for *β*-sheet, VAL_2 − NH ..... O − VAL_{13} pair at 300 K. The time scale for protein rupture in D_2O has a longer dissociation time and a stronger amplitude.

In the gas-phase simulation, although we simulate the α-helix, we observe the side chains to fold back and form internal hydrogen bonds, leading to an increase in the number of hydrogen bonds. However, in the water system, the hydrogen bond of the α-helix extrudes into water. Apparently, water softens the α-helix and more water−protein hydrogen bonds are generated. In this D_2O solvated system, for both α-helix and *β*-sheet, we found fewer hydrogen bonds formed (see Figure 3). This is consistent with the rmsd results.

In Figure 4, we show the rupture pattern for the protein in H_2O and D_2O. The hydrogen bond rupture process exhibits a clearer pattern in D_2O than that in H_2O. This also shows a strong suppression of the dynamic motion of the intraprotein hydrogen bond rupture processes. This agrees with a well structured D_2O network surrounding the protein with violent fluctuations.

We may think of the rupture processes in D_2O in the following two ways. First a stronger D-bond, as compared to an H-bond, wraps the protein more tightly. This can be illustrated via the root-mean-square derivative (rmsd) of a protein radius of gyration found for a simulation time up to 2 ns. In Figure 3, for three different temperatures, the protein rmsd in D_2O is always smaller than that in H_2O This means the protein is being wrapped tight in D_2O. Second the heavy mass of D_2O compared to H_2O, leads to a change in the rupture processes. To push out the H-bond of the protein into the solvent is more difficult in D_2O than in H_2O.

TABLE 2: Rupture Time (ps)

	in vacuum		in D_2O		in H_2O	
temp (K)	α-helix	*β*-hairpin	α-helix	*β*-hairpin	α-helix	*β*-hairpin
300	221.32		85.3	100.3	46	40
350	63.9	104	35.9	48	29	27.4
400	22.32	44				

Now let us turn to consider the molecular dynamics simulation results of the computer experiments in Table 1. After an Arrhenius fit of the rupture processes, we extract out the prefactor and activation enthalpy. The α-helix in the gas phase has essentially quite a large prefactor. However, for the solvated α-helix in H_2O, our previous work shows the existence of a water cavity similar to the clathrate hydrates. Due to this the prefactor is suppressed by 3 orders of magnitude. We therefore find a suppressed prefactor. The same is observed for the *β*-sheet as shown in Table 1. Here the corresponding rupture time is summarized in Table 2. Besides, the order of magnitude of both *A*-value and H_{BA}^{+} follows vacuum > D_2O > H_2O. The entropy effect is clearly explained by the larger *A*-value of the protein in D_2O, as compared to H_2O This supplements our argument of the free energy surface in Figure 1.

IV. Conclusion

We here show that the surrounding medium of D_2O has a profound effect on the H-bond in the protein structure. First, it slows down the rate substantially because the D_2O does not lower the activation energy for the hydrogen bond rupture as much as H_2O, which directly interacts with the hydrogen bond. Furthermore, the entropy term is severely suppressed as compared to H_2O. Hence D_2O inhibits dynamics functioning of the intraprotein hydrogen bond. Living creatures cannot survive in D_2O, and hence without H_2O there is no H-bond and no life. The activity of the same hydrogen bond cannot be maintained in the changed medium.

Now we extend our method of obtaining H-bond energies in proteins directly from a computer experiment that determines mean first passage times. These calculations show that H-bonds are strongly fluxional, much like water structures themselves

are fluxional. The effect of the H_2O structures on the H-bond is seen to reduce the H-bond energy quite strongly to a value now of importance in facilitating biological processes in water. However, in the opposite way, the entropy of the process is seen to be severely reduced, as one would expect for an H-bond breaking a well-ordered though fluctuating, very large water structure around the protein. This leads to a reduction in the rate by some 2 orders of magnitude just due to entropy alone—a sort of entropy bottle neck. This picture is corroborated by the results here in D_2O showing a strong influence of the medium on the strength of the hydrogen bond.

Therefore, the H-bond in proteins is here considered not as an atomistic motion but rather as imbedded in a collective motion of a very large water cluster in a fluxional equilibrium. Thus the energetics is reduced to the range of biological interest. D_2O, again working as a solvent, increases this energetic behavior by a factor of 2, which means that *RT* needs to be increased similarly. This again demonstrates the strong effect of the solvent on the hydrogen bond, but this is clearly too stringent a requirement for many life processes.

This global effect on the hydrogen bond would supposedly be finely tunable by additives and thus change the entropic or enthalpic moiety of the H-bond substantially[40]—even contributing to denaturation and grossly changing the flexibility and thus the reactivity of proteins.

Acknowledgment. S.-Y.S. and D.-Y.Y. gratefully thank the National Science Council of Taiwan in the Grant Nos. NSC-95-2113-M-010-001 and NSC-95-2113-M-001-013, respectively. We are grateful to the National Center for High-Performance Computing of Taiwan. This work was supported by the Taiwan/Germany program at the NSC/Deutscher Akademischer Austauschdienst. A portion of the research described in this paper was performed in the Environmental Molecular Sciences Laboratory, a national scientific user facility sponsored by the Department of Energy's Office of Biological and Environmental Research and located at the Pacific Northwest National Laboratory.

References and Notes

(1) Iavarone, A. T.; Patriksson, A.; van der Spoel, D.; Parks, J. H. *J. Am. Chem. Soc*. **2007**, *129*, 6726.
(2) Parker, M. J.; Clarke, A. R. *Biochemistry* **1997**, *36*, 5786.
(3) Cioni, P.; Strambini, G. B. *Biophys. J*. **2002**, *82*, 3246.
(4) Itzhaki, L. S.; Evans, P. A. *Protein Sci.* **1996**, *5*, 140.
(5) Schiffer, C. A.; Dotsch, V. *Curr. Opinion Biotechnol*. **1996**, *7*, 428.
(6) Stillinger, F. H. *Science* **1980**, *209*, 451.
(7) Guzzi, R.; Arcangeli, C.; Bizzarri, A. R. *Biophys. Chem.* **1990**, *82*, 9.
(8) Nielson, O. F.; Jacobsen, K. L.; Westh, P.; Radovic, T.; Larsen, B. D.; Christensen, D. H. *J. Mol. Struct.* **2001**, *598*, 9.
(9) Cui, Q.; Karplus, M. *J. Phys. Chem. B* **2003**, *107*, 1071.
(10) Efimova, Y. M.; Haemers, S.; Wierczinski. B.; Norde, W.; van Well, A. A. *Biopolymers* **2007**, *85*, 254.
(11) Eker, K.; Cao, X. L.; Nafie, L.; Huang, O. *J. Phys. Chem. B* **2003**, *107*,. 358.
(12) Unno, K.; Okada, S. *Plant Cell Physiol.* **1954**, *35*, 197.
(13) Connelly, P. R.; Aldape, R. A.; Bruzzese, F. J.; Chambers, S. P.; Fitzgibbon, M. J.; Fleming, M. A.; Itoh, S.; Livinston, D. J.; Navia, M. A.; Thomson, J. A.; Wilson, K. P. *Proc. Natl. Acad. Sci. U.S.A.* **1994**, *91*, 1964.
(14) Tarek, M.; Tobias, D. J. *Phys. Rev. Lett.* **2002**, *88*, 138101.
(15) Nemethy, G.; Scheraga, H. A. *J. Chem. Phys.* **1964**, *41*, 680.
(16) Guzzi, R.; Spartelli, L.; La Rosa, C.; Milardi, D.; Grasso, D. *J. Phys. Chem. B* **1998,** *102*, 2021.
(17) Makhatadze, G. I.; Clore, G. M.; Gronenburn, A. M. *Nat. Struct. Biol*. **1995**, *2*, 852.
(18) Laageand, D.; Hynesp, J. T. *Science* **2006**, *311*, 834.
(19) Cioni, P.; Strambini, G. B. *Biophys. J*. **2002**, *82*, 3246.
(20) Bhattacharya, S.; Bhandarkar, M. K.; Gaur, B. K. *Physiol. Plant.* **1969**, *22*, 1025.
(21) Gross, P. R.; Spindel, W. *Ann. N. Y. Acad. Sci.* **1960**, *90*, 500.
(22) Grigera, J. R. *J. Chem. Phys.* **2001**, *114*, 8064.
(23) Maybury, R. H.; Katz, J. J. *Nature* **1956**, *177*, 629.
(24) Borah, B.; Bryant, R. G. *Biophys. J*. **1982**, *38*, 47.
(25) Enright, J. T. *J. Comparative Physiol. A* **1971**, *72*, 1.
(26) Katz, J. J. *Sci. Am.* **1960**, *203*, 106.
(27) Smith, J. D.; Cappa, C. D.; Wilson, K. R.; Cohen, R. C.; Geissler, Ph. L.; Saykally, R. J. *Proc. Natl. Acad. Sci. U.S.A.* **2005**, *102*, 14171−14174.
(28) Glasstone, S.; Laidler, K. J.; Eyring, H. *The Theory of Rate Processes*; McGraw-Hill Book Co.: New York, 1941.
(29) Smith, J. D.; Cappa, C. D.; Wilson, K. R.; Cohen, R. C.; Geissler, P. L.; Saykally, R. J. *Proc. Natl. Acad. Sci. U.S.A.* **2005**, *102*, 14171.
(30) Eaves, J. D.; Loparo, J. J.; Fecko, C. J.; Roberts, S. T.; Tokmakoff, A.; Geissler, P. L. *Proc. Natl. Acad. Sci. U.S.A.* **2005**, *102*, 13019.
(31) Fersht, A. R.; Shi, Jian-Ping; Knill-Jones, J.; Lowe, D. M.; Wilkinson, A. J.; Blow, D. M.; Brick, P.; Carter, P.; Waye, M. M. Y.; Winter, G. *Nature* **1985**, *314*, 235.
(32) Kolano, C.; Helbing, J.; Kozinski, M.; Sander, W.; Hamm, P. *Nature* **2006**, *443*, 469.
(33) Davis, A. M.; Teague, S. J. *Angew. Chem., Int. Ed.* **1999**, *38*, 736.
(34) Davidson, D. W. *Clathrate hydrate* in *Water, A Comprehensive Treatise*; Frank, F., Ed.; Plenum: New York, 1973; Vol. 2, p 115.
(35) Sheu, Sheh-Yi; Yang, Dah-Yen; Selzle, H. L.; Schlag, E. W. *Proc. Natl. Acad. Sci, U.S.A.* **2003**, *100*, 12683.
(36) Kramers, H. A. *Physica* **1940**, *7*, 284.
(37) Brooks, B. R.; Bruccoleri, R. E.; Olafson, B. D.; States, D. J.; Swaminarhan, S.; Karplus, M. *J. Comput. Chem*. **1983**, *4*, 187.
(38) MacKerell, A. D., Jr.; Bashford, D.; Bellott, M.; Dunbrack, R. L., Jr.; Evanseck, J. D.; Field, M. J.; Fischer, S.; Gao, J.; Guo, H.; Ha, S.; Joseph-McCarthy, D.; Kuchnir, L.; Kuczera, K.; Lau, F. T. K.; Mattos, C.; Michnick, S.; Ngo, T.; Nguyen, D. T.; Prodhom, B.; Reiher, W. E., III; Roux, B.; Schlenkrich, M.; Smith, J. C.; Stote, R.; Straub, J.; Watanabe, M.; Wiorkiewicz-Kuczera, J.; Yin, D.; Karplus, M. *J. Phys. Chem. B* **1998**, *102*, 3586.
(39) Jorgensen, W. L.; Chandrasekhar, J.; Madura, J. D.; Impey, R. W.; Klein, M. L. *J. Chem. Phys.* **1983**, *79*, 926.
(40) Schwarzinger, S.; Wright, P. E.; Dyson, H. J. *Biochemistry* **2002**, *41*, 12681.